Upwelling characteristics in the Gulf of Finland (Baltic Sea) as revealed by Ferrybox measurements in 2007-2013

Villu Kikas, Urmas Lips

Marine Systems Institute at Tallinn University of Technology
Akadeemia tee 15a, 12618 Tallinn, Estonia
Tel: +3726204315, Fax: +3726204301
e-mail: villu.kikas@msi.ttu.ee

Abstract. Ferrybox measurements are carried out between Tallinn and Helsinki in the Gulf of Finland (Baltic Sea) on a regular basis since 1997. The system measures autonomously water temperature, salinity, chlorophyll *a* fluorescence and turbidity and takes water samples for further analyses at a predefined time interval. We aimed to show how the Ferrybox technology could be used to study the coastal upwelling events in the Gulf of Finland. Based on the introduced upwelling index and related criterion, 33 coastal upwelling events were identified in May-September 2007-2013. The number of events, as well as the frequency of their occurrence and intensity expressed as a sum of daily average temperature deviations in the 20-km wide coastal area, were almost equal near the northern and southern coast. Nevertheless, the wind impulse, which was needed to generate upwelling events of similar intensity, differed between the two coastal areas. It is suggested that the general thermohaline structure adapted to the prevailing forcing and the estuarine character of the basin weaken the upwelling created by the westerly-southwesterly (up-estuary) winds and strengthen the upwelling created by the easterly-northeasterly (down-estuary) winds. Two types of upwelling events were identified – one characterized by a strong temperature front and the other revealing gradual decrease of temperature from the open sea to the coastal area with maximum temperature deviation close to the shore.

Keywords: Ferrybox, coastal upwelling, upwelling index, cumulative wind stress, Gulf of Finland

32

1. INTRODUCTION

Unattended monitoring of marine environment using ships of opportunity has been implemented in many regions of the World Ocean (e.g. Paerl et al., 2009; Hardman-Mountford et al., 2008) including the Baltic Sea and the Gulf of Finland (Rantajärvi, 2003). The measurement systems installed on board commercial ferries or other ships are called "Ferryboxes" and they consist of various sensors, devices creating water flow through the sensors and software packages controlling the system and managing the data. The commonly used Ferryboxes measure temperature, salinity, and chlorophyll *a* fluorescence in the seawater pumped through the system from the surface layer along the ship track. First trials of using ships of opportunity for environmental monitoring in the Gulf of Finland were made by Estonian and Finnish scientists between Tallinn and Helsinki in 1990-1991 (Rantajärvi, 2003). Regular Ferrybox measurements along this route were started in 1997 while the longest data series of Ferrybox measurements (since 1993) is available along the ferry route Helsinki-Travemünde (Petersen, 2014).

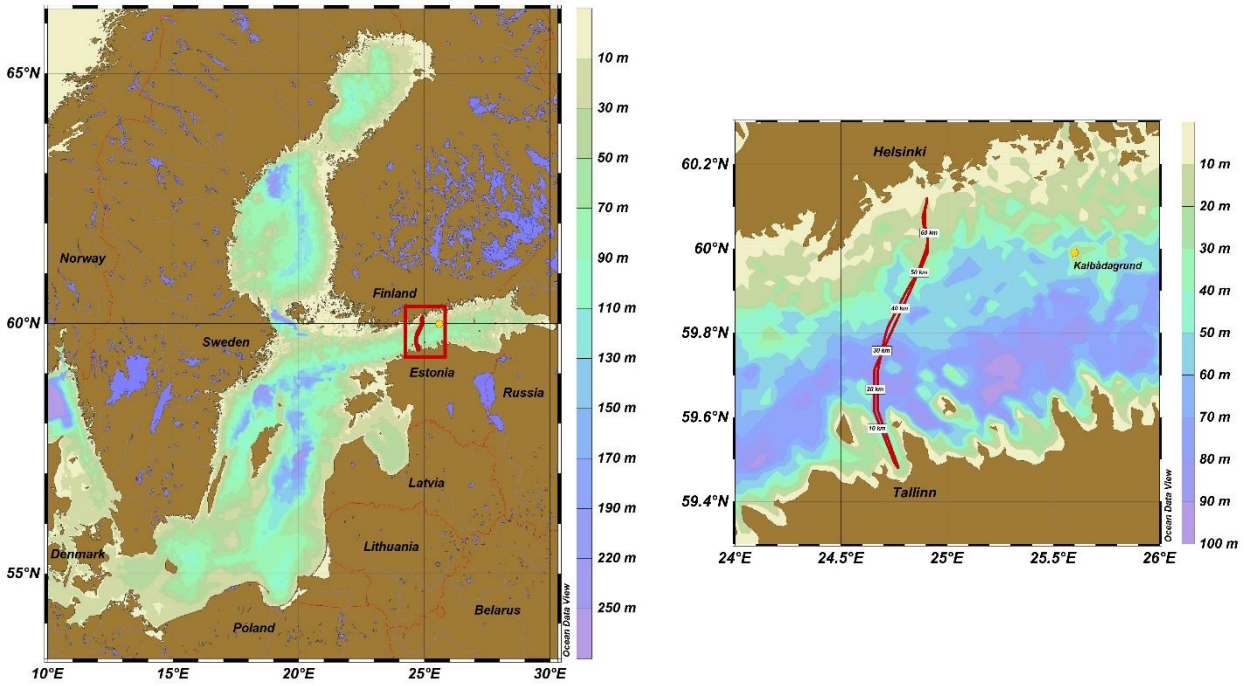

Figure 1. Map of the Baltic Sea (a) and the study area (b) with the Ferrybox transect and Kalbadagrund meteorological station.

The Gulf of Finland (GoF) lies in the northeastern part of the Baltic Sea (Fig. 1). It is an elongated basin with a length of about 400 km and a maximum width of 135 km (Alenius et al., 1998). The long-term residual circulation in the surface layer of the gulf is characterized by a relatively low speed and by a cyclonic pattern. The saltier water of the northern Baltic Proper flows into the gulf along the Estonian (southern) coast and the gulf water, which is less saline due to the large freshwater inflow at the eastern end of the gulf (the Neva River), flows out along the Finnish (northern) coast. The circulation is more complex at time scales from days to weeks mainly due to the variable wind forcing. A variety of mesoscale processes/features (fronts, eddies, upwelling/downwelling), which significantly affect the biological production, retention, and transport, have been observed in the Gulf of Finland (e.g. Talpsepp et al., 1994; Pavelson et al., 1997; Lips et al., 2009).

The vertical stratification in the gulf is characterized by a quasi-permanent halocline at the depths of 60-80 m, and a seasonal thermocline, which forms in spring-summer at the depths of 10-20 m (e.g. Liblik and Lips, 2011). While high concentrations of dissolved inorganic nitrogen (DIN) and phosphorus (DIP) are observed in winter, the concentrations of DIN and DIP are usually below the detection limit in summer in the upper mixed layer but still high just below the seasonal thermocline. In general, the most prominent features of the seasonal dynamics of phytoplankton in the Gulf of Finland are the spring bloom in April-May dominated by dinoflagellates/diatoms and the late summer bloom in July (or late June to mid-August) dominated by cyanobacteria (Kononen et al., 1996). However, the variations in bloom intensities and their spatial distributions are very high over the years and within the season that is often related to the physical forcing and especially to the mesoscale processes, including upwelling events (Lips and Lips, 2008; Vahtera et al., 2005).

Dynamics and characteristics of upwelling events have been studied in the Gulf of Finland based on in-situ measurements (e.g. Haapala, 1994), remote sensing (e.g. Uiboupin and Laanemets, 2009) and modeling (e.g. Myrberg and Andrejev, 2003). Most prominent upwelling events that were captured by measurements are an event along the northern coast in July 1999 (Vahtera et al., 2005) and an event along the southern coast in August 2006 (Lips et al., 2009). The following characteristic features of upwelling events in the Gulf of Finland are suggested:

1) the Finnish coastal sea in the north-western GoF is one of the main upwelling areas in the Baltic Sea (Myrberg and Andrejev, 2003) where upwelling frequency in May-September 1990-2009 has been up to 15% (Lehmann et al., 2012); almost the same upwelling frequency is suggested by the latter authors for the central GoF along the Estonian (southern) coast;
2) mean upwelling area detected on the basis of 147 maps during the period of 2000-2009 was 5642 km^2 (19% of the GoF surface area) along the northern coast and 3917 km^2 (13% of the GoF surface area) along the southern coast (Uiboupin and Laanemets, 2015), while the largest area covered by the upwelling water was identified as 12140 km^2 (data from 2000-2006; Uiboupin and Laanemets, 2009); the authors' estimate of the mean cross-shore extent of upwelling area was 20-30 km off the northern coast and varied between 7 and 20 km off the southern coast;
3) the intensity of upwelling events depends on the values of cumulative upwelling-favorable wind stress and strength of vertical stratification; Haapala (1994) suggested that at least 60 h long wind event has to exist to create an upwelling event; based on the wind data analysis from 2000-2005 and taking the threshold value for cumulative wind stress of 0.1 N m^{-2} d, on average, about 2 upwelling events should appear off the southern coast and 4 events off the northern coast (Uiboupin and Laanemets, 2009);
4) it is suggested that the difference in topography off the southern and northern coast of the GoF results in differing upwelling dynamics along the opposite coasts – in case of similar wind stress (but in opposite directions) the transport of waters from deeper layers starts earlier and is larger along the southern coast (Väli et al., 2011).

The motivation of the present paper is to show how the Ferrybox technology can be used to study mesoscale processes, especially coastal upwelling events in the Gulf of Finland. We describe the approach, its advantages and limits, and present statistical characteristics of upwelling events on the basis of data collected in 2007-2013. The main aim is to relate the observed variability and dynamics of upwelling events to the atmospheric forcing, reveal the differences in upwelling behavior in the two coastal areas and suggest an alternative physical

explanation of the found differences by taking into account the prevailing forcing and estuarine character of the basin.

2. THE MEASUREMENT SYSTEM AND METHODS

2.1. Ferrybox system

Temperature (T), salinity (S), chlorophyll *a* fluorescence and turbidity data and water samples for nutrients and phytoplankton chlorophyll *a* (Chl *a*), species composition and biomass analyses are collected unattended on passenger ferries, traveling between Tallinn and Helsinki (Fig. 1) since 1997. Due to the internal arrangements of the ferry company Tallink Silja and its predecessors, several ships were used as the platforms for Ferrybox measurements, which also differ regarding water intake features. A flow-through system from 4H-Jena, Germany with the water intake attached to the sea chest of the ferry is in use since 2006. The water enters the sea chest through a grating with a total surface area of 0.84 m^2 located at about 4 m depth below the waterline. The water flow from the sea chest into the system is forced by the hydrostatic pressure since the Ferrybox is located on the lower deck about 3 meters below the waterline. To restrict larger particles to get into the measurement system a mud filter (pore size 1 mm) is used close to the water intake. Before the sensors, a debubbler is installed to avoid air bubbles to affect the measurements of conductivity, turbidity and Chl *a* fluorescence. The flow rate through the sensors is stabilized by an internal pump, which is controlled by a pressure sensor in the system. Water samples are taken by a sampling device (Hach Sigma 900 MAX) whereas the water is pumped from the debubbler into the bottles using an internal pump of the water sampler.

For temperature measurements, a PT100 temperature sensor is used that is installed close to the water intake to diminish the effect of warming of water while flowing through the tubes onboard. The sensor has a measuring range from -2 to +40 °C and accuracy of ±0.1% of the range, thus 0.04 °C. For salinity measurements an FSI Excell thermosalinograph (temperature and conductivity meter) and for Chl *a* fluorescence and turbidity measurements a SCUFA submersible fluorometer (Turner Designs) with a flow-through cap is used. The system starts the measurements and data recording when the ferry is away from the harbor more than a predefined

distance of 0.7 nautical miles (controlled by a GPS device in the system) and stops when it is closer than this distance to avoid sediments getting into the system. The data are recorded during every crossing (twice a day) every 20 seconds that corresponds to a horizontal resolution of approximately 160 m.

2.2. Quality assurance and pre-processing of data

The sensors have been calibrated at the factory before the installation and if necessary sent for an additional laboratory calibration. Since the system contains two temperature sensors, the performance of them is routinely followed by a comparison of data acquired from the sensors. The quality of thermosalinograph data is guaranteed by taking a series of water samples (14-17 samples) and analyzing them using a high-precision salinometer AUTOSAL 2-4 times a year. The analyses have shown, that a correction of 0.08 (units in Practical Salinity Scale; the value has been stable over the years) must be added to the recorded salinity. While the raw salinity is recorded in units according to the Practical Salinity Scale 1978, the results on salinity distribution and variability are given later in this paper in g kg^{-1} (Sections 3 and 4). Particular care is taken to calibrate the SCUFA fluorometer; however, since we do not use the fluorometer data in this study the used routine is not described here.

The data acquired by the Ferrybox system recorded with a time step of 20 s are stored in an onboard terminal. To synchronize the measurements performed by the sensors having different sampling frequencies and GPS, the acquired data within every 19 s interval are averaged and recorded as measurements at every 20^{th} second. The data are automatically delivered to the on-shore FTP-server once a day when the ferry is in the harbor using a GSM connection. The performance of the system is validated by the control parameters, such as the flow rate and pressure in the system, and the data are checked for unrealistic values against the criteria set for every parameter on the basis of known natural variation of them in the Gulf of Finland.

One of the procedures, which has to be carried out when using the Ferrybox data, is the shifting of data points to the actual positions of the water intake. The problem arises since the coordinates attached to a data record correspond to the location of the ferry at the time of measurement, but

the water is taken in earlier at a different position. Since various systems of water intake are applied, this procedure is unique for each combination of a Ferrybox and a ferry. As described above, in our design the seawater enters first a relatively large sea chest and the flushing through time of it is unknown. While the water flows through the sea chest and into the tubes and debubbler with a flow rate of 12-15 l min^{-1}, the ferry moves on at an average speed of 16 knots. We solved the problem of position correction taking into account the advantage of having two crossings a day.

Analysis of data from forth and backward journeys allowed us to introduce a position correction procedure – the best result is achieved by shifting the measured data points against the GPS time for 3-4 minutes depending on the ferry and exact intake installation. This relatively long period is obviously related to the water exchange in the sea chest. Due to an almost constant cruising speed of the ferry outside the harbor areas, the applied procedure gives acceptable results. The comparison of data from Tallinn to Helsinki and back from Helsinki to Tallinn obtained on the same day is one of the used quality assurance procedures – the profiles containing unexpected deviations are marked by a quality flag indicating a possible quality problem.

2.3. Data and calculation methods

Temperature and salinity data collected along the ferry line Tallinn-Helsinki from May to September in 2007-2013 are used for analysis purposes. In 2008, the system on board the passenger ferry "Galaxy" was in use until 13 July and the measurements started again on 13 August when the system was installed on board the ferry "Baltic Princess". However, due to some technical problems, the regular measurements were successful from 2 September 2008. A failure of the system occurred late August 2012 and, therefore, the data are not available from 29 August until the end of September 2012. In early 2013, the next ferry ("Silja Europa") came to this line and the system was moved again causing a break in the measurements until 15 July 2013. The number of crossings with the full data coverage is given in Table 1. Four years – 2007, 2009, 2010 and 2011 – were the years with almost complete data coverage while most of the data were not available in the second half of July and August 2008, in September 2012 and in

May, June and the first half of July 2013. Thus, the data from all months from May to September were analyzed at least from six years in 2007-2013.

Collected raw data were preliminarily processed, including shifting of measurements as described in Section 2.2, quality checked and stored in the database. This data set was used to draw the maps of temporal variations of horizontal distributions of T and S for all studied years (Fig. 2). A step (cell width) of 0.5 km along the south-north oriented line was used to transform the data set from the matrix with a constant time step into the matrix with a constant spatial resolution. The fixed south-north orientation was applied to eliminate the influence of differences in orientation of the ship track in the southern, central and northern parts of the route (see Fig. 1) and of possible deviations from the ordinary route. As a result, the extent of the upwelling area is presented below in the south-north direction, and a coefficient has to be applied to convert these values to the upwelling extent in the cross-shore direction (as the cosine of the angle between the south-north direction and a perpendicular line to the shore – approximately 20 degrees).

An upwelling index was introduced in the coastal area off the southern coast (UI_S) and off the northern coast (UI_N). For each crossing, the average water temperature and horizontal profile of temperature deviations from the average were found. The upwelling index was calculated as a sum of negative temperature deviations in the 20-km coastal areas as:

$$UI_S = \sum_{\Delta T_i<0}^{i=1\ldots40}|\Delta T_i| \text{ and } UI_N = \sum_{\Delta T_i<0}^{i=101\ldots140}|\Delta T_i| \quad (1)$$

where ΔT_i is the temperature deviation at 0.5-km cell *i* from the average temperature of the crossing. The width of 20 km was selected on the basis of the analysis of all available temperature data from Tallinn-Helsinki ferry line in 2007-2013 (see Section 3.1 for details). The daily indexes were obtained by averaging the two upwelling indexes from a single day (from forth and backward journey of the ferry). The cumulative upwelling index (*CUI*) can be calculated by summing up upwelling index values for certain periods. The obtained *CUI* values were divided by 40, which is the number of data cells in the 20-km wide coastal area, to keep the meaning of *CUI* as the sum of average negative temperature deviations, having a unit of [°C day]:

$$CUI_S(n1 \ldots n2) = \sum_{j=n1}^{j=n2}\left(\frac{1}{40}UI_{Sj}\right) \text{ and } CUI_N(n1 \ldots n2) = \sum_{j=n1}^{j=n2}\left(\frac{1}{40}UI_{Nj}\right) \quad (2)$$

where *n1* and *n2* are the start and the end day number of the selected period, for which the cumulative upwelling index is calculated, and UI_{Sj} and UI_{Nj} are the upwelling indexes at day *j* off the southern and northern coast, respectively. This approach of the *CUI* calculation is similar to those used previously in the studies of upwelling events and their influence on the phytoplankton dynamics in the Gulf of Finland (see e.g. Lips and Lips, 2008; Myrberg et al., 2008).

An upwelling event can be characterized by the cumulative upwelling index whereas the first and the last day of the event can be defined as the start and end of the period when the upwelling index (UI_N or UI_S) exceeded a certain threshold value. We have defined this threshold value as 40 °C, which corresponds e.g. to a 20-km wide upwelling with an average negative temperature deviation of 1 °C. This choice is explained in more detail in Section 3.2. The accuracy of the temperature sensor of 0.04 °C gives a maximum uncertainty of 1.6 °C in the upwelling index estimates (since it is a sum of 40 temperature values – 40*0.04 °C). It is 25 times less than the selected threshold for the upwelling detection (40 °C).

Wind data were obtained from the HIRLAM (High-Resolution Limited Area Model) version of the Estonian Meteorological and Hydrological Institute with the spatial resolution of 11 km and the time interval of 3 h (Väli, 2011; Männik and Merilain, 2007). Model data point close to Kalbådagrund, where also a meteorological weather station is located (Finnish Meteorological Institute), was chosen to represent the wind conditions in the study area. The data from Kalbådagrund weather station or the closest HIRLAM model point have also been used in the earlier studies of coastal upwellings in the Gulf of Finland (Lips et al., 2008a; Uiboupin and Laanemets, 2009). According to Keevallik and Soomere (2010), the HIRLAM output matches well with the observations at Kalbådagrund (the wind is measured at 32 m), although the modeled wind direction (at 10 m height) is turned by 20° counter-clockwise from the measured wind direction.

Wind stress (in N m^{-2}) is calculated for the wind component along the axis of the Gulf of Finland, which corresponds to the direction turned by 70 degrees clockwise from the north direction, as:

$$\tau_{70} = C_D \rho_a |U| U_{70} \quad (3)$$

where U is the wind speed (in m s^{-1}), U_{70} is its component in the along-gulf direction, C_D is the drag coefficient (a value of 1.2 10^{-3} was chosen in the present study), and ρ_a is the air density (1.2 kg m^{-3}). Accordingly, positive values of the wind stress should initiate southward Ekman transport in the surface layer and vice versa. The cumulative wind stress (in N m^{-2} day) was calculated based on daily averages of wind stress. If the cumulative wind stress is large enough, upwelling events occur along the northern coast in case of the positive wind stress and along the southern coast in case of the negative wind stress.

3. RESULTS

3.1 General variability and distribution patterns

The typical seasonal trend of the surface layer temperature in the Gulf of Finland is characterized by temperature about 5 °C at the beginning of May, a maximum > 20 °C in late July – early August and a drop below 15 °C in late September. Within the analyzed years 2007-2013, the surface layer temperature was the highest in summer 2010 (Fig. 2) when the period with the average along-transect temperature > 20 °C was 35 days. On the background of seasonal trend and simultaneous shorter-term increases or decreases of temperature over the whole study transect, the periods with distinctly lower temperature were observed off the northern or southern shore. Such situations are related to the coastal upwelling events – their characteristic time scale was several days to 1-2 weeks, and they extended towards the open sea by 15-20 km (Fig. 2).

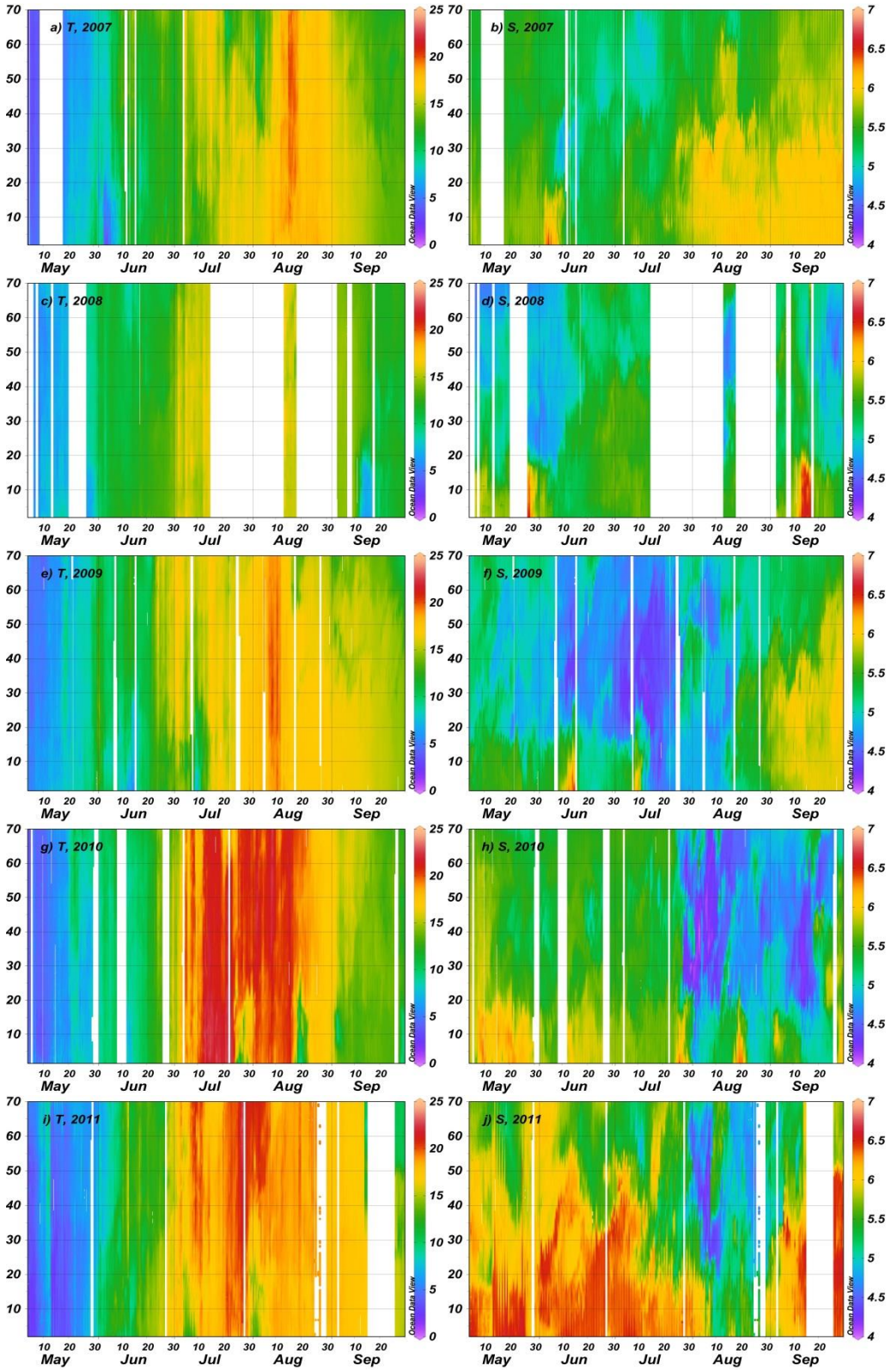
a) T, 2007
b) S, 2007
c) T, 2008
d) S, 2008
e) T, 2009
f) S, 2009
g) T, 2010
h) S, 2010
i) T, 2011
j) S, 2011
May
Jun
Jul
Aug
Sep
Ocean Data View

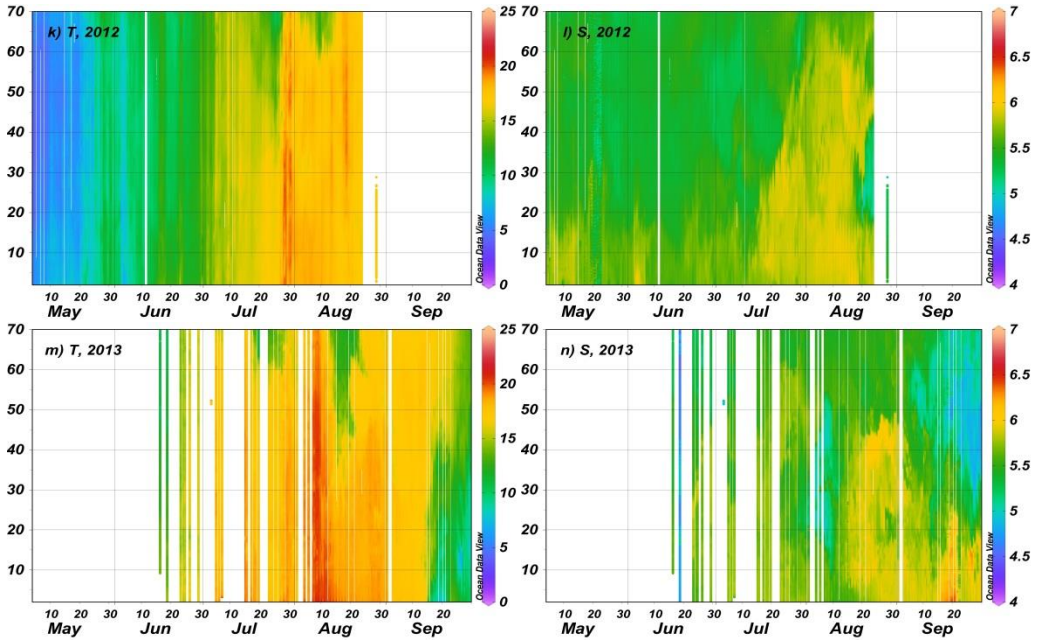

293

294

295 **Figure 2. Temporal changes in temperature (in °C) and salinity (in g kg $^{-1}$) distributions between Tallinn and Helsinki from 1 May to 30**
296 **September in 2007 (a, b), 2008 (c, d), 2009, (e, f), 2010 (g, h), 2011 (i, j), 2012 (k, l) and 2013 (m, n); y-axis shows the distance from the Tallinn**
297 **Bay (latitude 59.48 N) in km along the meridional transect.**

298

299 Inter-annual variations of the surface layer salinity in 2007-2013 were high with the highest
300 salinity in 2011 and the lowest in 2009. The surface layer salinity exceeded 6.5 g kg^{-1} for a
301 longer period only in 2011 in the southern half of the study transect (Fig. 2j) and for shorter
302 periods of several days in case of coastal upwelling events off the southern shore (e.g. Figs. 2b
303 and 2d). Note that in the case of coastal upwelling events seen in the temperature distributions
304 off the northern coast, a simultaneous increase in salinity was not well visible. As a rule, the
305 surface layer salinity was higher near the southern coast than that near the northern coast.
306 However, often the lowest salinity was measured in the middle of the transect – it means in the
307 open sea areas (e.g. Figs. 2f and 2h). Seasonal trend of salinity differed between the studied years
308 remarkably. While usually, the lowest surface layer salinity was observed in June-July, in 2008,
309 the salinity was the lowest in May, and in 2010 and 2011, it was the lowest in August.

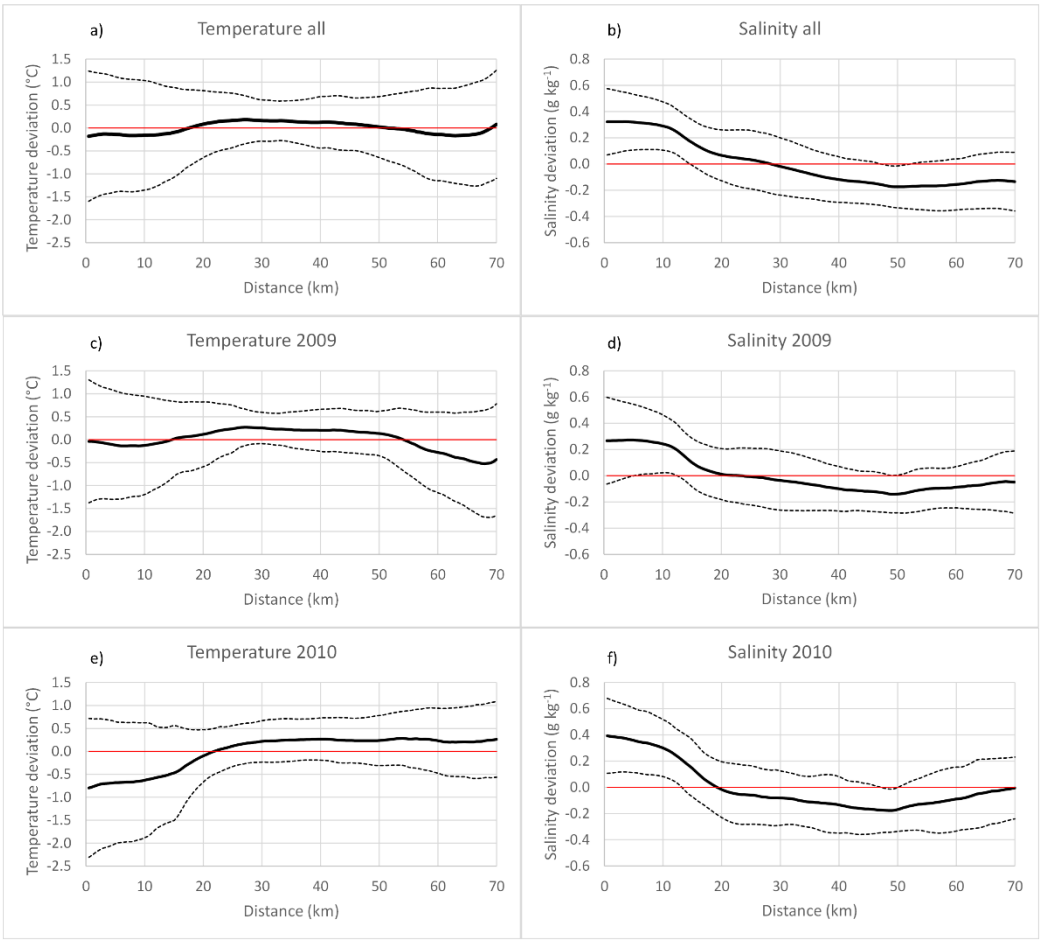

Figure 3. Distributions of temperature (in °C) and salinity (in g kg $^{-1}$) deviations from the transect mean value along the ferry route Tallinn-Helsinki for all measurements in May-September 2007-2013 (a, b), 2009 (c, d) and 2010 (e, f). Mean values for each 0.5-km cell (solid curves) and plus/minus RMSE (dashed curves) are shown; x-axis indicates the distance from the Tallinn Bay (latitude 59.48 N) in km along the meridional transect.

The average temperature and salinity deviations in May-September each year and for the entire study period, as well as their root mean square errors (RMSE), were calculated in each 0.5-km cell. On average, the temperature deviations were close to zero along the entire study transect (Fig. 3a) – the absolute values of average deviation were six times less than estimated RMSE of temperature. Nevertheless, the surface layer temperature was slightly warmer in the open Gulf of Finland than in approximately 20-km wide coastal areas (Fig. 3a). This result could be related to the coastal upwelling events. For instance, in 2009, when coastal upwelling events were observed off the both coasts, the average temperature deviations were negative near the both coasts (Fig. 3c). In 2010, when upwelling events occurred mostly off the southern coast, the

negative values of average temperature deviations were detected only in the southern part of the transect (Fig. 3e).

It is remarkable that, on average, the variability of temperature deviations was much higher near the coasts than in the central part of the study transect (Fig. 3a). In the case of upwelling events off the southern coast and their absence off the northern coast (in 2010), this high variability of temperature was concentrated only in the 20-km wide coastal area off the southern shore (Fig. 3e). Since the area of the high variability of temperature, which mostly could be related to the upwelling activity, extended about 20 km from the shores, it was suggested to estimate the intensity of upwelling events based on data from these 20-km wide coastal zones.

The average distribution of the surface layer salinity along the transect was characterized by higher salinity values in the southern gulf and lower values in the northern gulf (Fig. 3b). The salinity deviations were positive in the 28-km wide area off the southern coast (with clearly higher salinity in the first 10 km) and negative along the rest of the study transect. However, the minimum of the surface layer salinity was observed at about 20 km from the northern shore (or at a distance of 50 km from the southern end of the study transect) almost in every year (Fig. 3b, d, and f). The only exception was the year 2007 when the lowest salinity was observed on average in the cell closest to the northern shore. The low salinity water at the distance of 50 km indicates that, in summer, the outflow of the less saline Gulf of Finland surface waters occurs mostly in the northern part of the open gulf. The spatial differences in variability of the surface layer salinity were not so distinct than in variability of the surface layer temperature. One can recognize slightly higher variability (RMSE) of the surface layer salinity in the coastal areas and the southern part of the open gulf at the distance of 20-30 km.

3.2 Upwelling characteristics

As it is seen on the maps of temperature deviations (Fig. 4), the years 2007 and 2009 had a similar pattern – the upwelling events occurred off the southern coast in the first half of the season and off the northern coast in the second half. In 2008, upwelling events were observed near the southern coast in May and September, and they appeared near the northern coast in

June. The year 2010 was an exceptional year when the upwelling events occurred mostly along the southern coast. It was exceptional also because the sea surface temperature outside the upwelling waters was the highest among the studied summers. A sequence of consecutive upwelling events near the northern and southern coast was observed in 2011. Upwelling events occurred mostly off the northern coast in 2012 and 2013.

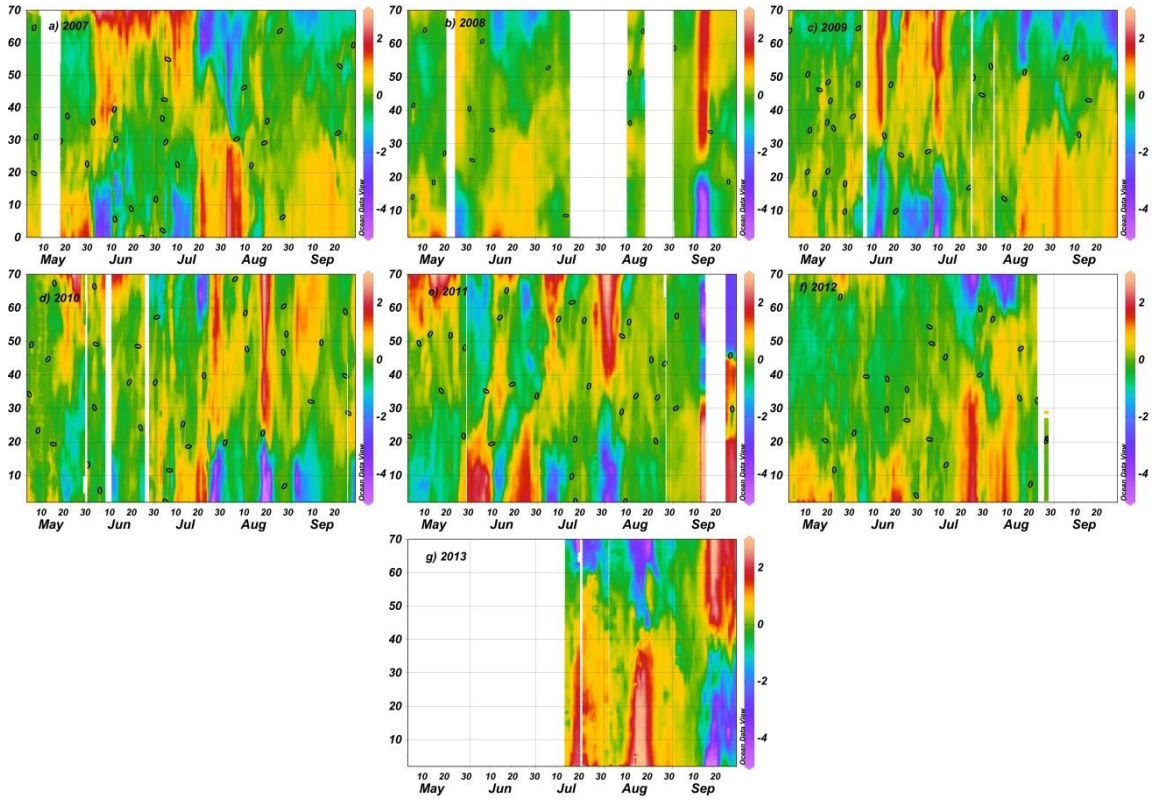

Figure 4. Temporal changes in spatial distributions of temperature deviations (in °C) from the daily transect mean value between Tallinn and Helsinki from 1 May to 30 September in 2007 (a), 2008 (b), 2009, (c), 2010 e), 2011 (f), 2012 (g) and 2013 (h); y-axis shows the distance from the Tallinn Bay (latitude 59.48 N) in km along the meridional transect.

We selected a criterion to detect whether an upwelling event occurs or not as the value of the upwelling index (*UI*) exceeding 40 °C (in absolute values while *UI* is by definition a negative number). The upwelling events found using the selected criterion were also the occasions when the maximum negative temperature deviation from the transect mean value was at least -2 °C (except one event on 10-17 September 2007 when the maximum deviation was -1.97 °C). Furthermore, no other cases with negative temperature deviations exceeding -2 °C were detected.

Thus, the criterion *UI* < -40 °C gives quite similar results as would yield if using the criterion based on the maximum negative temperature deviation of -2 °C.

We identified in May-September 2007-2013 altogether 33 upwelling events, approximately half of them (17) near the northern coast and half (16) near the southern coast (Table 2). The events lasted from 3 days to 3 weeks, and the longest event was observed on 11-31 August 2013. On average five events yearly were registered, and the maximum number of events (eight) was observed in 2011. Based on available data, the number of days with the upwelling near the northern coast was 150 and near the southern coast 140. As the total number of days with measurements was 838, the upwelling occurred on 18 % and 17 % of days off the northern and southern coast, respectively. The maximum negative temperature deviation from the mean value was detected in August 2010 near the southern coast when it reached -7.78 °C. The largest temperature deviation in the case of upwelling events near the northern coast of -6.15 °C was detected in July 2013. The average of maximum temperature deviation was larger for the upwelling events near the southern coast than near the northern coast (-4.64 °C and -3.60 °C, respectively).

While the maximum temperature deviation characterizes the peak of the upwelling, the introduced cumulative upwelling index also takes into account the extent of the upwelling in space and time. Regarding *CUI* the largest upwelling events were observed in 2013 – on 15-30 September 2013 off the southern coast (*CUI* = -40.2 °C day) and on 11-31 August 2013 off the northern coast (*CUI* = -39.7 °C day). The upwelling events with the largest temperature deviation in July-August 2010 were relatively short events lasting 7 days and gave respective *CUI* value as -15.7 °C day and -20.8 °C day. The average *CUI* value of all upwelling events off the northern coast was -14.5 °C day and off the southern coast -16.2 °C day. The sum of *CUI* values of all detected upwelling events off the northern coast was -247.0 °C day and off the southern coast -258.4 °C day.

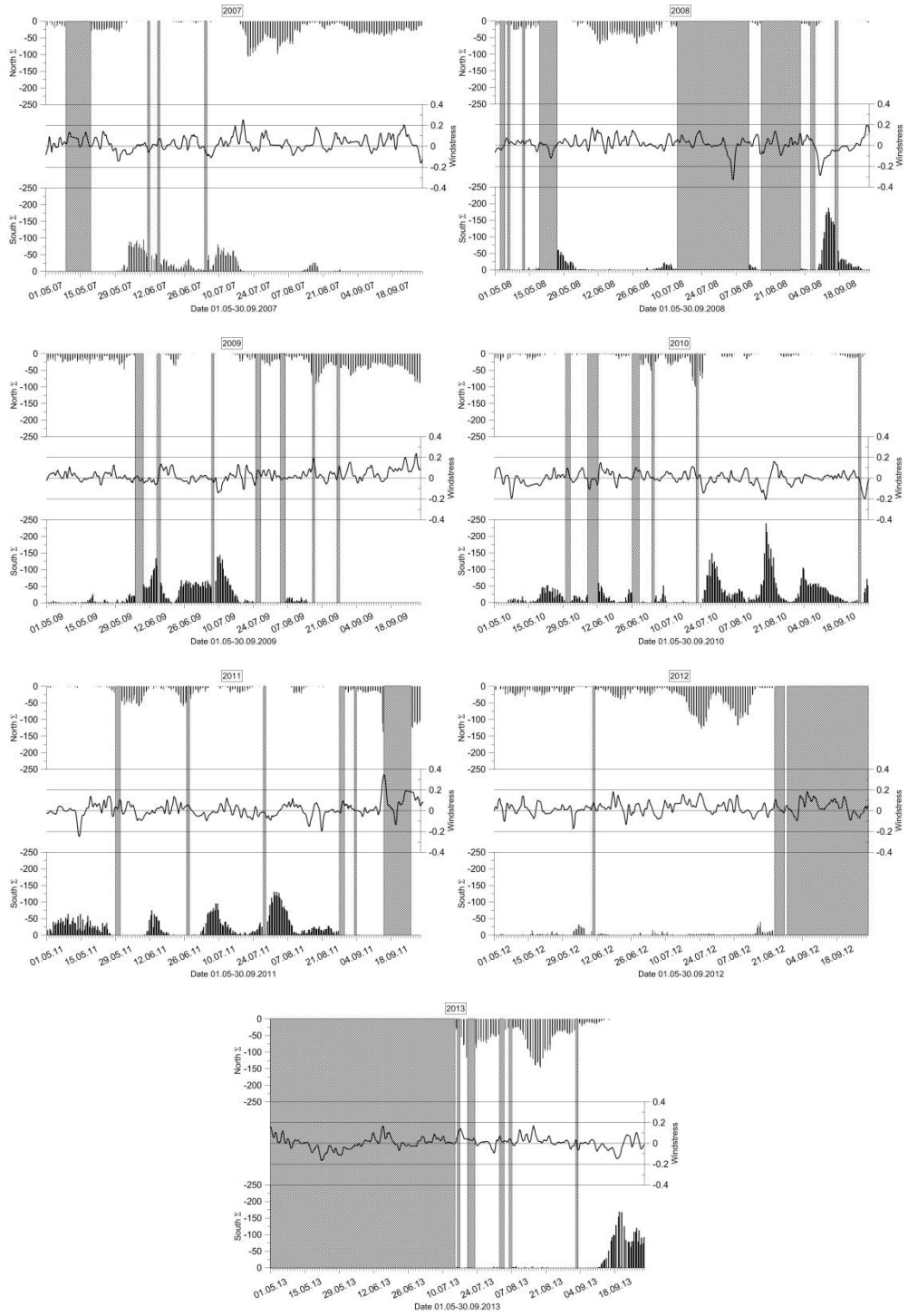

Figure 5. Temporal changes in upwelling index off the northern coast (at the top of each subplot; °C) and off the southern coast at the bottom of each subplot; °C) and along-gulf wind stress (black curve in the middle; N m^{-2}) in May-September 2007 (a), 2008 (b), 2009 (c), 2010 (d), 2011 (e), 2012 (f) and 2013 (g).

The total *CUI* for all measurement days in 2007-2013 was -405.3 °C day for the northern coastal area and -356.6 °C day for the southern coastal area. Thus, the negative temperature deviations from the transect mean were more common for the northern coastal sea area while the upwelling events were more intense in the southern coastal sea area. This feature is also well seen in Fig. 5 where e.g. in 2007 relatively low values of UI_N were found in most of the days near the northern coast but only three upwelling events were revealed according to the criterion set in the present study.

Seasonal variation of the frequency of occurrence and intensity of upwelling events based on the analyzed data is as it follows. The highest number of events was observed in July – 10 events, 5 off the northern coast and 5 off the southern coast, and the lowest in May – 4 events. The sum of *CUI* values of all events in July and August were -185.3 °C day and -187.9 °C day, respectively, while it was only -28.6 °C day in May. In June and September, the *CUI* of all events had intermediate magnitude -107.5 °C day and -137.0 °C day, respectively. Obviously, the revealed seasonal trend was partly related to the temperature difference between the surface layer and the cold layer beneath the seasonal thermocline, which has its maximum in the Gulf of Finland in July-August (Liblik and Lips, 2011).

3.3 Upwelling characteristics in relation to wind forcing

The occurrence of coastal upwelling events in the Gulf of Finland can be related quite well to the variations of the along-gulf wind stress (Fig. 5). The upwelling events appeared after a certain favorable wind pulses with long enough duration and magnitude. In the case of upwelling events off the northern coast, the positive along-gulf wind stress was usually observed a few days before the event and in the case of upwelling events off the southern coast, the wind stress was negative for a few days (Fig. 5).

The estimated cumulative wind stress for the detected upwelling events varied between 0.31 and 1.37 N m^{-2} day for westerly winds and between -0.09 and -1.08 N m^{-2} day for easterly winds (Table 2). The cumulative wind stress associated with each upwelling event was calculated based on daily average wind stress values by summing them up from the first day with favorable wind

stress (within a period of 1 week before the event) to the last day with favorable wind stress before the end of the event. If only one day with opposite wind stress appeared in a sequence in the favorable wind stress series, then the calculation period was not broken. The average value of the cumulative wind stress for an upwelling event off the northern coast was 0.71 N m^{-2} day and off the southern coast -0.44 N m^{-2} day. It suggests that to produce a coastal upwelling event of an equal magnitude the required favorable along-gulf wind stress has to be larger for the upwelling events off the northern coast than for the events off the southern coast. This conclusion is drawn by taking into account the above result that the average upwelling intensity (estimated as *CUI*) was similar for the both coastal areas with slightly higher values of *CUI* for the upwelling events off the southern coast. This suggestion is also supported by comparison of relationships between the *CUI* and cumulative wind stress (*CWS*) related to the upwelling events near the opposite coasts (Fig. 6). The linear regression lines between the *CUI* and *CSW* indicate that at the same *CSW* values, the upwelling events had higher intensities off the southern coast than off the northern coast. Nevertheless, the results are quite scattered, and the coefficient of determination (r^2) between the *CUI* and *CSW* are 0.30 for the southern and 0.19 for the northern upwelling events.

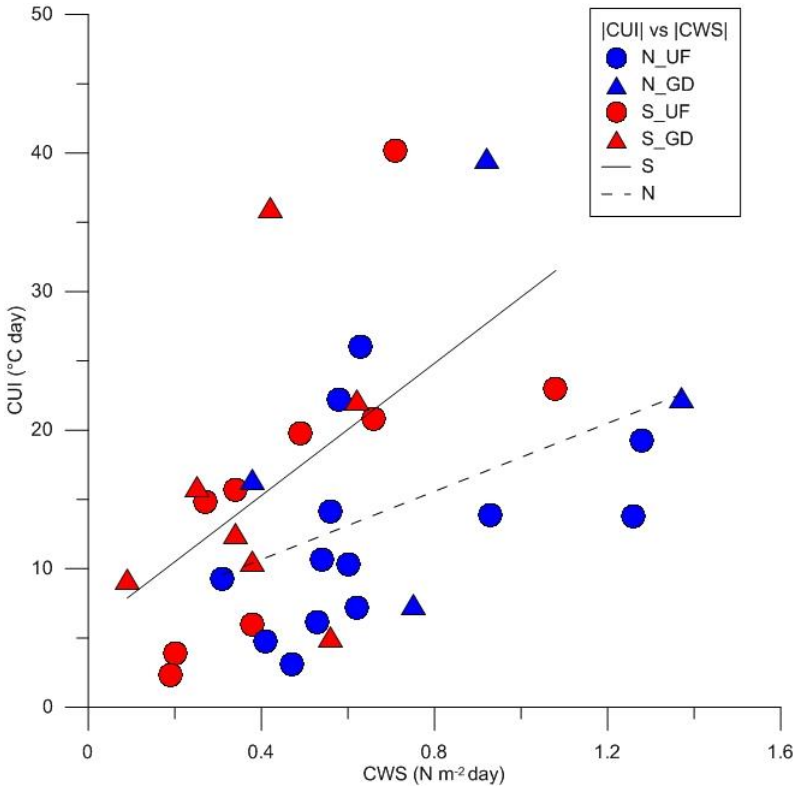

Figure 6. The relationship between the cumulative upwelling index (CUI) and cumulative along-gulf wind stress (CWS) based on 33 detected upwelling events in May-September 2007-2013. Red symbols indicate the events off the southern coast and blue symbols the events off the northern coast; circles correspond to the events with pronounced upwelling front (N_UF and C_UF) and triangles the events with a gradual decrease in temperature towards the coast (N_GD and S_GD). The linear regression lines for southern (solid line) and northern upwelling events (dashed line) are shown.

The average along-gulf wind stress for the entire study period from May to September in 2007-2013 was 0.016 N m^{-2}. The seasonal averages had positive values in all studied years indicating that the westerly-south-westerly winds prevailed in the region. The average values of wind stress varied between 0.001 N m^{-2} in 2010 and 0.029 N m^{-2} in 2007, 2009 and 2012. In May-September 2010, when five upwelling events occurred off the southern coast and only one event off the northern coast, the average along-gulf wind stress was close to zero indicating that the cumulative wind forcing was almost equal from both directions. Furthermore, the wind stress averaged over all observed upwelling events in 2007-2013 was 0.015 N m^{-2}, which is very close to the average wind stress over the entire study period. This estimate was obtained based on the mean length of upwelling events of 8.8 days and mean cumulative wind stress values of 0.71 and -0.44 N m^{-2} day off the northern and southern coasts, respectively. It can be concluded that the difference between the wind impulses needed for the generation of upwelling events with similar intensity near the opposite coasts is comparable to the average wind stress value in the region.

Usually, the upwelling events occurred one or a few days after the start of the favorable wind pulse, and the maximum of upwelling intensity was reached one or a few days after the maximum wind stress (Fig. 5). We made an attempt to reveal characteristic spatial temperature and salinity distributions in the surface layer from coast to coast at times of the maximum intensity of upwelling events. Surprisingly, the results did not differ significantly between the northern and southern coast – two characteristic shapes of upwelling events in the temperature distribution were identified for both coastal areas.

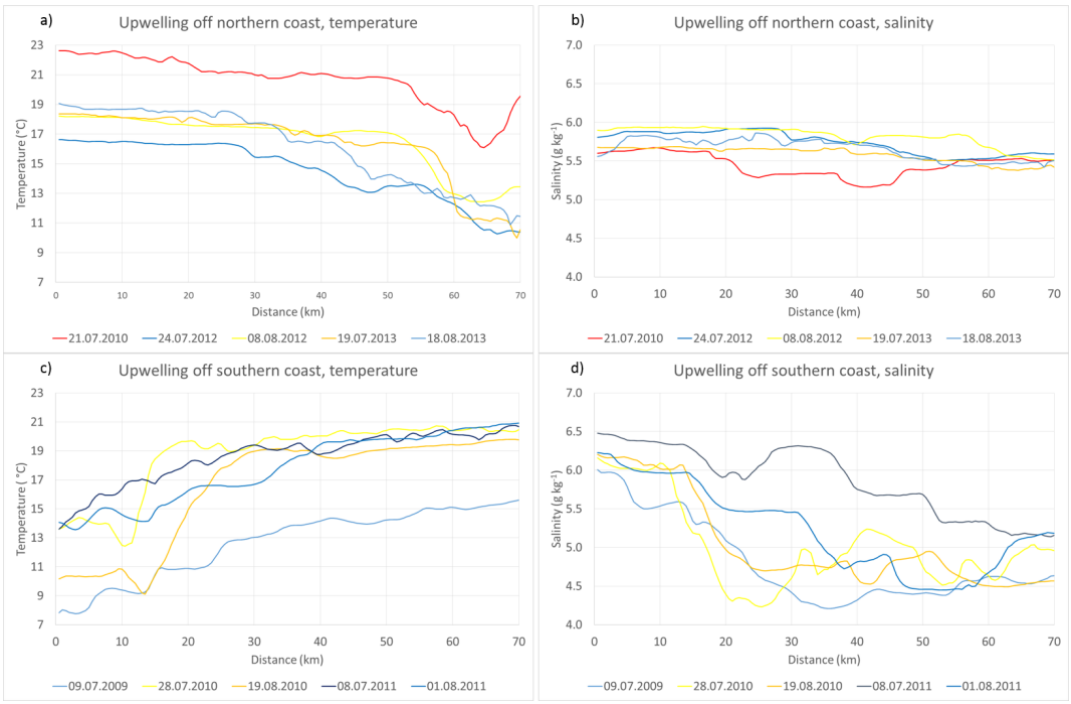

Figure 7. Characteristic distributions of temperature and salinity along the ferry route Tallinn-Helsinki with coastal upwelling events off the northern coast (a, b) and off the southern coast (c, d); x-axis shows the distance from the Tallinn Bay (latitude 59.48 N) in km along the meridional transect.

Mostly the upwelling events were characterized by a sharp and very intense temperature front between the upwelling waters and the rest of the transect (see Fig. 7 the yellow and orange curves). Typical for such events were an almost uniform temperature outside the upwelling area and the temperature minimum (maximum temperature deviation) close to the upwelling front. The other distribution pattern (blue curves in Fig. 7) exposed a gradual decrease of temperature towards the upwelling waters. Typical for the latter events were the irregularities in temperature distribution with a characteristic scale of a few kilometers and the temperature minimum (maximum temperature deviation) in the cell closest to the shore. In some cases, e.g. the event near the northern coast with maximum intensity on 18 August 2013 (see the light blue curve in Fig. 7 upper left panel), the observed temperature deviations were as large as during the upwelling events with strong temperature front. There was also a third type of temperature distribution when the upwelling waters were not attached to the shore (see red curve in Fig. 7 upper left panel) at least according to the measurements along the ferry route. All these types of upwelling events are well recognized on the maps of temporal changes of temperature and temperature deviation along the ferry route Tallinn-Helsinki (Figs. 2 and 4).

The spatial distribution of salinity in the surface layer from coast to coast drastically differed between the upwelling events near the northern coast and the events near the southern coast (Fig. 7 right panels). In the latter case, both the salinity difference across the gulf and the spatial variability at scales of a few to ten kilometers were much larger than in the former case. It is also interesting that in the case of southern upwelling events, the salinity minimum along the transect can be situated either very close to the upwelling front (e.g. on 28 July 2010) or near the northern coast (e.g. 8 July 2011). Although such diverse patterns are partly related to the history of water movements in the gulf, the salinity minimum (at least local minimum) close to the upwelling front obviously is caused by the westward current jet along the front as also revealed by model experiments (Laanemets et al., 2011). The salinity distribution across the gulf associated with the northern upwelling events is very uniform with some variability at scales of a few to ten kilometers, which have the amplitude several times less than spatial salinity variations associated with the southern upwelling events.

4. DISCUSSION

Several studies have shown how the Ferrybox measurements are successfully used for different applications, such as for monitoring of coastal waters in combination with remote sensing (Petersen et al., 2008), estimating carbon fluxes and primary productivity (Schneider et al., 2014) and detecting cyanobacterial blooms (Seppälä et al., 2007). However, not enough attention is paid to the Ferrybox systems, especially to the question how the results are affected by the used technical solutions (like water intake depth and construction, piping, etc.). Furthermore, the particularities of geographical location as well as the ferry route and schedule often determine the most suitable applications and requirements for the data treatment. A good example of taking advantage of the geographical location and ferry route is demonstrated by Buijsman and Ridderinkhof (2007) who estimated the water and suspended matter exchange between the Wadden Sea and the North Sea using data collected along the ferry route Den Helder – Texel.

The ferry route between Tallinn and Helsinki across the elongated Gulf of Finland and the schedule consisting of two cruises a day and a short 1.5-hour stay in Helsinki made it possible to

introduce a procedure for correction of coordinates of measurement points and an additional quality check routine for the collected data. The correlation between the data from the two crossings on the same day should be high enough; otherwise, the data can be marked as suspicious. We found that the highest correlation between the two datasets is achieved when the data points are shifted by 3-4 minutes depending on the intake installation and the ferry. This analysis also demonstrates the confidence of the applied Ferrybox system even though the water is taken in through a relatively large sea chest. Furthermore, the ferry route across the relatively narrow gulf from coast to coast is very convenient to collect data on the offshore extension and intensity of coastal upwelling events.

Various methods have been applied to reveal characteristic features of coastal upwelling events in the Baltic Sea based on data mainly from remote sensing and numerical models. Data of high-resolution long-term Ferrybox measurements have not been analyzed with this aim until now. Certain temperature isoline as the border of the upwelling area was used by Uiboupin and Laanemets (2009) and a temperature deviation (2 °C) from the mean temperature along zonal transects was employed by Lehmann et al. (2012). The latter method is similar to the approach applied in the present study, but we argue that the analysis of temperature deviations along meridional transects is more appropriate in the Gulf of Finland. This conclusion is justified by the fact that, on average, the north-south temperature gradient is negligible in the gulf (see Fig. 3a) while the west-east temperature gradient could exist between the shallower and narrower Gulf of Finland and the deeper and wider Northern Baltic Proper due to differential warming and cooling.

Nevertheless, it is interesting that our results on upwelling frequencies of about 17-18 % near the northern and southern coast are very close to the results of Lehmann et al. (2012) if their results based on remote sensing data were considered. They concluded that upwelling events were present more than 15 % of time near the northern coast and about 15 % of time near the southern coast. At the same time, the estimates of corresponding upwelling frequencies based on numerical experiments differ from the values obtained from the remote sensing data and the results of the present study. Based on model results, the northern coastal area has been suggested as the main upwelling area in the Gulf of Finland with the upwelling occurrence up to 30 % of

time (Lehmann et al., 2012; Myrberg and Andrejev, 2003) while near the southern coast downwelling should prevail (e.g. Myrberg and Andrejev, 2003). It shows that the models with their current resolution and parameterization of sub-grid processes should be improved.

Analysis of wind data has also suggested that the coastal upwelling events should occur more often off the northern coast of the Gulf of Finland than off the southern coast (Lehmann et al., 2012; Uiboupin and Laanemets, 2009). The data set consisting of 838 days of measurements from coast to coast used in the present analysis has revealed that, on average, the frequency of upwelling events and their intensity are similar near the northern and southern coast of the gulf although the wind data from the same period suggest prevalence of upwelling events off the northern coast. Partly, this outcome can be explained by the higher position of the thermocline, steeper bottom slope and greater depths in the southern part of the gulf as suggested by some earlier studies (e.g. Väli et al., 2011; Laanemets et al. 2009). Based on a simple theory of upwelling dynamics linking the position of the onshore return flow with the bottom slope and stratification (Lentz and Chapman, 2004), Laanemets et al. (2009) estimated that the return flow should occur in the near-bottom layer for both northern and southern upwelling events in the Gulf of Finland. Due to the steeper slope and greater depths, the upwelling outcome in the vertical transport of cold and nutrient rich waters could be more intense in the southern gulf (Väli et al., 2011; Laanemets et al., 2009).

An alternative explanation could be suggested if taking into account the estuarine character of the Gulf of Finland – the basin has free water exchange with the Baltic Proper in the west while it is closed in the east where the main freshwater source is located. First, this basin configuration and the prevalence of southwesterly winds together with the Coriolis force cause a general cyclonic circulation in the surface layer of the gulf (Alenius et al., 1998). Such circulation, in accordance with the geostrophic balance, yields in a higher sea level and deeper thermocline at the northern part of the gulf (e.g. see Andrejev et al., 2004). A similar suggestion was made by Liblik and Lips (2016) when they analyzed the relationship between the cross-gulf inclination of the thermocline and wind forcing based on data from 35 cross-gulf CTD surveys conducted in 2006-2013. Thus, the wind impulse needed for the initiation of a coastal upwelling event near the southern coast can have a smaller magnitude. This suggestion is supported by the comparison of

603 the lowest cumulative wind stress values, which have initiated upwelling events in 2007-2013
604 near the two costs. The lowest *CWS* value related to an upwelling event along the northern coast
605 is larger than the *CWS* values for five upwelling events along the southern coast (see Fig. 6).
606
607 Secondly, we suggest that for a stronger wind impulse during a longer period, the estuarine
608 character of the basin has a significant influence on the outcome. If the strong southwesterly
609 winds prevail, a downward movement of the thermocline in the gulf as a whole occurs since the
610 southwesterly winds cause inflow in the surface layer and outflow in the sub-surface layers (see
611 e.g. Elken et al., 2003; Lips et al., 2008b). In contrary, the down-estuary winds cause a general
612 upward movement of the thermocline in the gulf. Consequently, the up-estuary southwesterly
613 winds, on the one hand, cause upwelling along the northern coast, but on the other hand
614 downwelling in the gulf as a whole that could weaken the outcome. In the case of the down-
615 estuary easterly-northeasterly winds, a general upward movement of the thermocline in the gulf
616 supports the coastal upwelling along the southern coast. Such response of the water movements
617 to the forcing could be an explanation why, in general, the cumulative upwelling indexes
618 (presented in Fig. 6) increase faster with the strengthening of the favorable wind stress (*CWS* in
619 Fig. 6) for the southern upwelling events than for the northern upwelling events.
620
621 The average cross-gulf distributions of temperature and salinity were described based on the 7-
622 year data set of horizontal profiles. On average, the surface layer temperature did not have any
623 horizontal gradient while the surface layer salinity was higher in the southern part than in the
624 northern part of the gulf. The result that the surface water with the lowest salinity was on average
625 at about 20 km from the northern coast supports the suggested general circulation scheme in the
626 Gulf of Finland (e.g. Andrejev et al., 2004). At the same time, if the wind forcing favorable for
627 upwelling events near the southern coast prevailed (as it was observed in summer 2010) the low
628 salinity water appeared in the southern part of the open gulf, close to the upwelling front. This
629 phenomenon was also observed during an intense upwelling event in August 2006 (Lips et al.,
630 2009); it was modeled by Laanemets et al. (2011) and noted by Liblik and Lips (2016) based on
631 an analysis of CTD data from surveys across the gulf in 2006-2013.
632

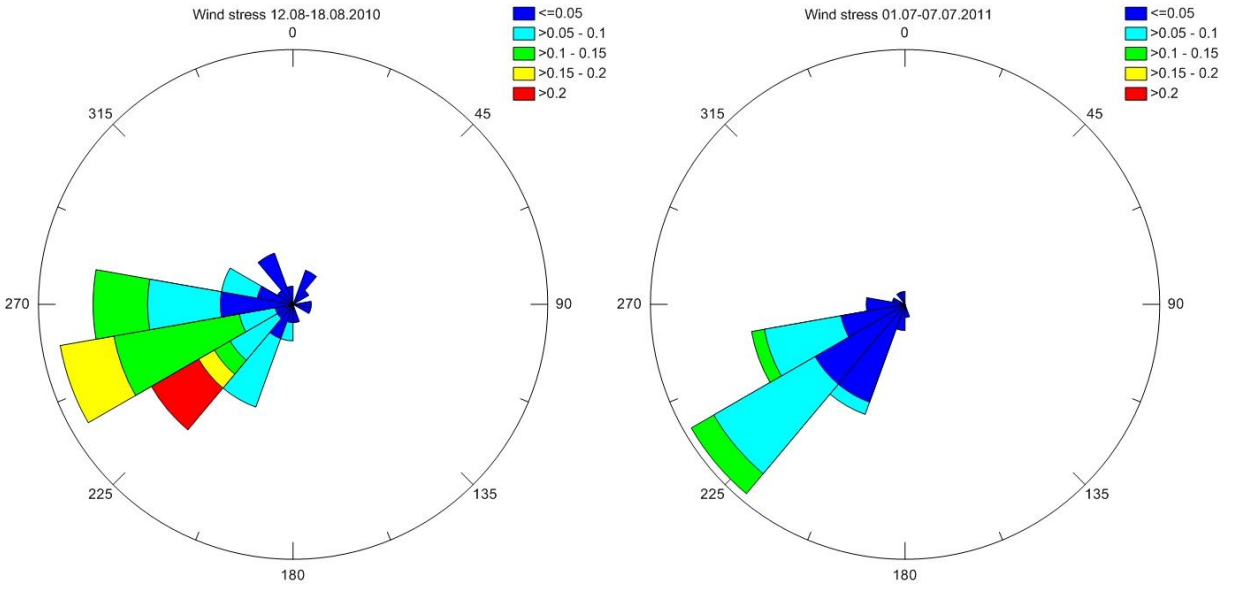

633
634 **Figure 8. Polar histogram of wind stress vectors (N m^{-2}) based on the wind data from a weekly period before the peak of upwelling events off**
635 **the Estonian coast on 17-23 August 2010 (left panel) and 5-11 July 2011 (right panel).**

636

637 The most intense upwelling events regarding temperature deviations were observed near the
638 southern coast as it was also found by Uiboupin and Laanemets (2009, 2015). However, we did
639 not identify clear differences in the temperature distribution patterns between the upwelling
640 events off the two coasts. Instead, near the both coasts, the classical distribution with a sharp
641 temperature front as well as the distribution characterized by a gradual decrease in temperature
642 towards the coast have been observed. We suggest that the latter type of temperature distribution
643 could be associated with the development of upwelling filaments, which occurred and stayed in
644 our measurement window for the several observed upwelling events.

645

646 In the case of the upwelling events along the southern coast, the wind speed was on average
647 higher before the events with the sharp temperature front (see Fig. 6 and Table 2). For instance,
648 the polar histograms of wind stress vectors shown in Fig. 8 are very similar except the
649 distribution of wind stress magnitudes. The period before the culmination of the upwelling event
650 with the sharp temperature front observed on 19 August 2010 had a large share of wind stress
651 values > 0.15 N m^{-2}. Nevertheless, the two prominent upwelling events along the northern coast
652 – the most intense event (on 11-31 August 2013) and the event corresponding to the largest

cumulative wind stress (on 18-27 July 2012), were both characterized by the gradual decrease in temperature towards the coast (Fig. 6).

The filaments of upwelled waters are characteristic features of the upwelling events in the Gulf of Finland (Uiboupin and Laanemets, 2009). Zhurbas et al. (2008) have shown based on a numerical experiment that the cold/warm water squirts and filaments could develop after the weakening of the upwelling favorable winds. Similarly, the squirts and filaments could develop if the wind forcing is strong enough to initiate an upwelling event but not as strong as needed to retain the mesoscale frontal dynamics. In the case of the southern upwelling events, it explains why upwelling events with the gradual decrease of temperature mostly occurred when the wind forcing was on average weaker.

As shown by Zhurbas et al. (2006), the baroclinic instability of the upwelling jet is expected to occur when the bottom slope is smaller than the isopycnal slope. Thus, for the strong upwelling events, the filaments might appear with a higher probability in the case of northern upwelling events since the bottom slope is about two times shallower in the northern gulf than in the southern gulf (Uiboupin and Laanemets, 2009). Furthermore, the probability of filament formation could be higher when the thermocline had a deeper position that might enhance the influence of the bottom irregularities to the upwelling dynamics. The prevailing westerly-southwesterly winds, which cause an inflow in the upper layer and a compensating outflow in the deeper layers (Elken et al., 2003; Liblik and Lips, 2012), could lead to the deepening of the seasonal thermocline in the gulf in 2012 and 2013. The two very intense upwelling events with the gradual temperature decrease were observed in these summers along the northern coast. Since the upwelling dynamics is dependent on the vertical structure of the water column before the event (e.g. Lentz and Chapman, 2004), these suggestions have to be studied further in the future by combining Ferrybox data (restricted to the surface layer and single transect) with the remote sensing and water column data.

5. CONCLUSIONS

We showed that Ferrybox data from the Tallinn-Helsinki ferry route could be successfully employed to describe the characteristics of coastal upwelling events in the Gulf of Finland. An advantage of the geographical location of the ferry route across the relatively narrow gulf and the schedule consisting of two crossings a day allowed to control the quality of the data and introduce the upwelling index based on the data from a single crossing and the cumulative upwelling index. In total, 33 coastal upwelling events were identified in May-September 2007-2013. It is shown that the upwelling occurrences of 18 % and 17 % of days, as well as intensities of upwelling events, are similar near the northern and southern coast. The most intense events occur in July-August, most probably because of the warmest surface layer (strongest thermocline) during those months. It is shown that the wind impulse needed to generate upwelling events of similar intensity differs between the two coastal areas. We suggest that the general thermohaline structure (adapted to the prevailing forcing) and the estuarine character of the basin are reasons for the found different outcome. The thermohaline structure of the Gulf of Finland is characterized by a deeper position of the thermocline in the northern gulf; thus, the upwelling initiation requires a stronger wind impulse there than in the southern coastal area. Furthermore, the estuarine character of the basin leads to the weakening of the upwelling created by the westerly (up-estuary) winds and strengthening of the upwelling created by the easterly (down-estuary) winds. Two types of upwelling events were identified – one characterized by a strong temperature (upwelling) front and the other revealing gradual decrease of temperature from the open sea to the coastal area with maximum temperature deviation very close to the shore. We suggest that the spatial variations in temperature with scales of a few kilometers, which were characteristic for the latter type of upwelling events, could be signs of the meso- and sub-mesoscale features (filaments and squirts) associated with the upwelling dynamics.

Acknowledgements

We are grateful to Tallink (Estonia) for the possibility to conduct the measurements on board the ferries. We thank our colleagues, especially Inga Lips and Fred Buschmann, for their help in maintaining the Ferrybox system, and Taavi Liblik for his suggestions regarding data processing. This work was supported by institutional research funding IUT19-6 of the Estonian Ministry of Education and Research and by EU Regional Development Foundation, Environmental

714 Conservation and Environmental Technology R&D Programme project VeeOBS (3.2.0802.11-
715 0043).
716
717 **References**
718
719 Alenius, P., Myrberg, K., Nekrasov, A. 1998. The physical oceanography of the Gulf of Finland:
720 a review. *Boreal Environ. Res.*, 3, 97–125.
721 Andrejev, O., Myrberg, K., Alenius, P., Lundberg, P.A., 2004. Mean circulation and water
722 exchange in the Gulf of Finland - a study based on three-dimensional modeling. *Boreal*
723 *Environ. Res.*, 9(1), 1–16.
724 Buijsman, M.C., Ridderinkhof, H., 2007. Long-term ferry-ADCP observations of tidal currents
725 in the Marsdiep inlet. *J. Sea Res.*, 57, 237–256.
726 Elken, J., Raudsepp, U., Lips, U., 2003. On the estuarine transport reversal in deep layers of the
727 Gulf of Finland. J. Sea Res. 49, 267–274.
728 Haapala, J. 1994. Upwelling and its influence on nutrient concentration in the coastal area of the
729 Hanko Peninsula, entrance of the Gulf of Finland. *Est. Coast. Shelf Sci.*, 38(5), 507–521.
730 Hardman-Mountford, N. J., Moore, G., Bakker, D. C. E., Watson, A. J., Schuster, U., Barciela,
731 R., Hines, A., Moncoiffe´, G., Brown, J., Dye, S., Blackford, J., Somerfield, P. J., Holt,
732 J., Hydes, D. J., and Aiken, J. 2008. An operational monitoring system to provide
733 indicators of CO2- related variables in the ocean. – *ICES Journal of Marine Science*, 65,
734 1498–1503.
735 Keevallik, S., Soomere, T., 2010. Towards quantifying variations in wind parameters across the
736 Gulf of Finland. *Estonian Journal of Earth Sciences*, 59(4), 288–297.
737 Kononen, K., Kuparinen, J., Mäkela, K., Laanemets, J., Pavelson, J., Nõmmann, S., 1996.
738 Initiation of cyanobacterial blooms in a frontal region at the entrance to the Gulf of
739 Finland, Baltic Sea. *Limnol. Oceanogr.*, 41, 98–112.
740 Laanemets, J., Väli, G., Zhurbas, V., Elken, J., Lips, I., Lips, U., 2011. Simulation of mesoscale
741 structures and nutrient transport during summer upwelling events in the Gulf of Finland
742 in 2006 *Boreal Environ. Res.*, 16A, 15–26.

743 Laanemets, J., Zhurbas, V., Elken, J., Vahtera, E., 2009. Dependence of upwelling-mediated
744 nutrient transport on wind forcing, bottom topography and stratification in the Gulf of
745 Finland: model experiments. *Boreal Environ. Res.*, 14, 213–225.
746 Lehmann, A., Myrberg, K., Höflich, K., 2012. A statistical approach to coastal upwelling based
747 on the analysis of satellite data for 1990-2009. *Oceanologia*, 54, 369-393.
748 Lehmann, A., Myrberg, K., 2008. Upwelling in the Baltic Sea – A review. *J. Marine Syst.*, 74,
749 S3–S12.
750 Lentz, S.J., Chapman, D.C., 2004. The importance of nonlinear cross-shelf momentum flux
751 during wind-driven coastal upwelling. *J. Phys. Oceanogr.*, 34, 2444–2457.
752 Liblik, T., Lips, U., 2016. Variability of pycnoclines in a three-layer, large estuary: the Gulf of
753 Finland. *Boreal Environ. Res.* (in press).
754 Liblik, T., Lips, U., 2012. Variability of synoptic-scale quasi-stationary thermohaline
755 stratification patterns in the Gulf of Finland in summer 2009. *Ocean Sci*., 8, 603–614.
756 Liblik, T., Lips, U., 2011. Characteristics and variability of the vertical thermohaline structure in
757 the Gulf of Finland in summer. *Boreal Environ. Res*., 16A, 73–83.
758 Lips, I., Lips, U. 2008. Abiotic factors influencing cyanobacterial bloom development in the
759 Gulf of Finland (Baltic Sea). *Hydrobiologia*, 614, 133–140.
760 Lips, I., Lips, U., Liblik, T. 2009. Consequences of coastal upwelling events on physical and
761 chemical patterns in the central Gulf of Finland (Baltic Sea). *Cont. Shelf Res.* 29, 1836–
762 1847.
763 Lips, U., Lips, I., Kikas, V., Kuvaldina, N., 2008a. Ferrybox measurements: a tool to study
764 meso-scale processes in the Gulf of Finland (Baltic Sea). *US/EU-Baltic Symposium,*
765 *Tallinn, 27-29 May, 2008. IEEE, (IEEE Conference Proceedings)*, 1 - 6.
766 Lips, U., Lips, I., Liblik, T., Elken, J., 2008b. Estuarine transport versus vertical movement and
767 mixing of water masses in the Gulf of Finland (Baltic Sea). *US/EU-Baltic Symposium,*
768 *Tallinn, 27-29 May, 2008. IEEE, (IEEE Conference Proceedings)*, 1 - 8.
769 Männik, A., Merilain, M., 2007. Verification of different precipitation forecasts during extended
770 winter-season in Estonia. *HIRLAM Newsletter*, No. 52, 65–70.
771 Myrberg, K., Lehmann, A., Raudsepp, U., Szymelfenig, M., Lips, I., Lips, U., Matciak, M.,
772 Kowalewski, M., Krezel, A., Burska, D., Szymanek, L., Ameryk, A., Bielecka, L.,
773 Bradtke, K., Galkowska, A., Gromisz, S., Jedrasik, J., Kaluzny, M., Kozlowski, L.,

774 Krajewska-Soltys, A., Oldakowski, B., Ostrowski, M., Zalewski, M., Andrejev, O.,
775 Suomi, I., Zhurbas, V., Kauppinen, O.-K., Soosaar, E., Laanemets, J., Uiboupin, R.,
776 Talpsepp, L., Golenko, M., Golenko, N., Vahtera, E., 2008. Upwelling events, coastal
777 offshore exchange, links to biogeochemical processes – Highlights from the Baltic Sea
778 Science Congress at Rostock University, Germany, 19-22 March 2007. *Oceanologia*, 50,
779 95-113.
780 Myrberg, K., Andrejev, O. 2003. Main upwelling regions in the Baltic Sea – a statistical analysis
781 based on three-dimensional modeling. *Boreal Environ. Res.*, 8(2), 97-112.
782 Paerl, H.W., Rossignol, K.L., Guajardo, R., Hall, N.S., Joyner, A., Peierls, B.L., Ramus, J.S.
783 2009. FerryMon: Ferry-Based Monitoring and Assessment of Human and Climatically
784 Driven Environmental Change in the Albemarle-Pamlico Sound System. *Environ. Sci.*
785 *Technol.*, 43, 7609–7613
786 Pavelson, J., Laanemets, J., Kononen, K., S. Nõmman, 1997. Quasi-permanent density front at
787 the entrance to the Gulf of Finland: Response to wind forcing. *Cont. Shelf Res.*, 17, 253-
788 265.
789 Petersen, W., 2014. FerryBox systems: State-of-the-art in Europe and future development. *J.*
790 *Marine Syst.*, 140, 4-12.
791 Petersen W., Wehde, H., Krasemann, H., Colijn, F., Schroeder, F., 2008. FerryBox and MERIS –
792 Assessment of coastal and shelf sea ecosystems by combining in situ and remotely sensed
793 data. *Est. Coast. Shelf Sci.*, 77, 296-307.
794 Rantajärvi, E. (Ed.) 2003. Alg@line in 2003: 10 years of innovative plankton monitoring and
795 research and operational information service in the Baltic Sea. *MERI – Report Series of*
796 *the Finnish Institute of Marine Research*, No. 48, 1-36.
797 Schneider, B., Gülzow, W., Sadkowiak, B., Rehder, G., 2014. Detecting sinks and sources of
798 CO2 and CH4 by ferrybox-based measurements in the Baltic Sea: Three case studies. *J.*
799 *Marine Syst.*, 140, 13-25.
800 Seppälä, J., Ylöstalo, P., Kaitala, S., Hällfors, S., Raateoja, P., Maunula, P., 2007. Ship-of-
801 opportunity based phycocyanin fluorescence monitoring of the filamentous cyanobacteria
802 bloom dynamics in the Baltic Sea. *Est. Coast. Shelf Sci.*, 73, 489-500.

Talpsepp, L., Nõges, T., Raid, T., Kõuts, T. 1994. Hydrophysical and hydrobiological processes in the Gulf of Finland in summer 1987 – characterization and relationship. *Cont. Shelf Res.*, 14, 749-763.

Uiboupin, R., Laanemets, J., 2009. Upwelling characteristics derived from satellite sea surface temperature data in the Gulf of Finland, Baltic Sea, *Boreal Environ. Res.*, 14 (2), 297-304.

Uiboupin, R., Laanemets, J., 2015. Upwelling parameters from bias-corrected composite satellite SST maps in the Gulf of Finland (Baltic Sea). *IEEE Geoscience and Remote Sensing Letters*, 12, 592-596.

Vahtera, E., Laanemets, J., Pavelson, J., Huttunen, M., Kononen, K., 2005. Effect of upwelling on the pelagic environment and bloom-forming cyanobacteria in the Western Gulf of Finland, Baltic Sea. *J. Marine Syst.*, 58, 67-82.

Väli, G., 2011. Numerical experiments on matter transport in the Baltic Sea. PhD thesis, Tallinn Technical University Press.

Väli, G., Zhurbas, V., Laanemets, J., Elken, J., 2011. Simulation of nutrient transport from different depths during an upwelling event in the Gulf of Finland. *Oceanologia*, 53, 431-448.

Zhurbas, V., Laanemets, J., Vahtera, E., 2008. Modeling of the mesoscale structure of coupled upwelling/downwelling events and the related inputs of nutrients to the upper mixed layer in the Gulf of Finland, Baltic Sea. *J. Geophys. Res.*, 113, C05004, doi: 10.1029/2007JC004280.

Zhurbas, V.M., Oh, I.S., Park, T., 2006. Formation and decay of a longshore baroclinic jet associated with transient coastal upwelling and downwelling: a numerical study with application to the Baltic Sea. *J. Geophys. Res.*, 111, C04014, doi: 10.1029/2005JC003079.

Table 1. Periods of measurements along the ferry route Tallinn-Helsinki in 2007-2013, number of days with measurements and number of days with upwelling events off the northern coast (N) and off the southern coast (S).

Year	Ferry	Period	Number of days with data	Number of days with upwelling	
				N	S
2007	Galaxy	1 May – 30 September	141	26	21
2008	Galaxy Baltic Princess	1 May – 13 July 13 August – 30 September	90	8	11
2009	Baltic Princess	1 May – 30 September	145	33	30
2010	Baltic Princess	1 May – 30 September	140	5	32
2011	Baltic Princess	1 May – 30 September	135	19	30
2012	Baltic Princess	1 May – 28 August	113	22	0
2013	Silja Europa	15 July – 30 September	74	37	16

Table 2. Characteristics of detected upwelling events; dates, coastal area (N – off northern coast; S – off southern coast), type (UF – with strong upwelling front, GD - - with gradual decrease of temperature), maximum temperature deviation from the transect mean value, cumulative upwelling index calculated for each event and cumulative along-gulf wind stress calculated for upwelling favourable winds before and during the upwelling event.

No	Dates	Coast	Type	Maximum temperature deviation (°C)	Cumulative upwelling intensity (°C day)	Cumulative wind stress (N m^{-2} day)
1.	3-14 June 2007	S	UF	-4.12	-19.8	-0.49
2.	8-16 July 2007	S	GD	-3.02	-12.6	-0.34
3.	21-27 July 2007	N	UF	-4.02	-13.9	0.93
4.	29 July – 8 August 2007	N	GD	-3.64	-16.5	0.38
5.	10-17 September 2007(1)	N	GD	-1.97	-7.5	0.75
6.	26-28 May 2008(2)	S	UF	-2.52	-3.9	-0.20
7.	11-15 June 2008	N	UF	-2.73	-7.2	0.62
8.	27-29 June 2008	N	UF	-2.27	-6.2	0.53
9.	10-17 September 2008	S	UF	-5.42	-23.0	-1.08
10.	9-16 June 2009	S	UF	-4.77	-14.8	-0.27
11.	24 June – 14 July 2009	S	GD	-5.78	-36.1	-0.42
12.	16-22 August 2009	N	UF	-3.20	-10.7	0.54
13.	28 August – 9 September 2009	N	UF	-2.74	-14.1	0.56

14.	17-30 September 2009[3]	N	UF	-3.09	-19.3	1.28
15.	20-24 May 2010	S	GD	-2.21	-5.1	-0.56
16.	12-13 June 2010[4]	S	UF	-2.60	-2.3	-0.19
17.	20-24 July 2010	N	UF	-4.70	-9.3	0.31
18.	26 July – 1 August 2010	S	UF	-6.19	-15.7	-0.34
19.	17-23 August 2010	S	UF	-7.78	-20.8	-0.66
20.	2-12 September 2010	S	GD	-5.27	-16.0	-0.25
21.	4-12 May 2011[5]	S	GD	-2.22	-9.3	-0.09
22.	31 May – 8 June 2011	N	UF	-2.32	-10.3	0.60
23.	11-15 June 2011	S	UF	-3.12	-6.0	-0.38
24.	24-27 June 2011	N	UF	-2.40	-4.8	0.41
25.	5-10 July 2011	S	GD	-5.05	-10.6	-0.38
26.	29 July – 7 August 2011	S	GD	-4.69	-22.2	-0.62
27.	14 September 2011[6]	N	UF	-4.90	-3.1	0.47
28.	26-30 September 2011[7]	N	UF	-3.27	-13.8	1.26
29.	18-27 July 2012[8]	N	GD	-4.55	-22.4	1.37
30.	2-13 August 2012	N	UF	-4.17	-22.2	0.58
31.	17 July – 1 August 2013[9]	N	UF	-6.15	-26.0	0.63
32.	11-31 August 2013	N	GD	-5.03	-39.7	0.92
33.	15-30 September 2013	S	UF	-7.34	-40.2	-0.71

[1] temperature deviation was less than -2 °C during the event on 10-17 September 2007
[2] data absent before 26 May 2008 for more than 1 day
[3] data analysed until 30 September 2009 (upwelling event did further)
[4] data absent before 12 June 2010 for more than 1 day
[5] early spring with possible contribution of difference in surface water warming
[6] no data available after 14 September 2011
[7] no data available before 26 September 2011, wind data missing on 24-26 September 2011
[8] wind data on 14-15 July 2012 not available
[9] ferrybox data on 20-21 July 2013 not available

Figure captions

Figure 1. Map of the Baltic Sea (a) and the study area with the Ferrybox transect and Kalbadagrund meteorological station.

Figure 2. Temporal changes of temperature (in °C) and salinity (in g kg^{-1}) distributions between Tallinn and Helsinki from 1 May to 30 September in 2007 (a, b), 2008 (c, d), 2009, (e, f), 2010 (g, h), 2011 (i, j), 2012 (k, l) and 2013 (m, n); y-axis shows the distance from the Tallinn Bay (latitude 59.48 N) in km along the meridional transect.

Figure 3. Distributions of temperature (in °C) and salinity (in g kg^{-1}) deviations from the transect mean value along the ferry route Tallinn-Helsinki for all measurements in May-September 2007-2013 (a, b), 2009 (c, d) and 2010 (e, f). Mean values for each 0.5-km cell (solid curves) and plus/minus RMSE (dashed curves) are shown; x-axis shows the distance from the Tallinn Bay (latitude 59.48 N) in km along the meridional transect.

Figure 4. Temporal changes of spatial distributions of temperature deviations (in °C) from the daily transect mean value between Tallinn and Helsinki from 1 May to 30 September in 2007 (a), 2008 (b), 2009, (c), 2010 e), 2011 (f), 2012 (g) and 2013 (h); y-axis shows the distance from the Tallinn Bay (latitude 59.48 N) in km along the meridional transect.

Figure 5. Temporal changes of upwelling index off the northern coast (at the top of each subplot; °C) and off the southern coast (at the bottom of each subplot, °C) and along-gulf wind stress (black curve in the middle; N m^{-2}) in May-September 2007 (a), 2008 (b), 2009 (c), 2010 (d), 2011 (e), 2012 (f) and 2013 (g).

Figure 6. Relationship between the cumulative upwelling index (CUI) and cumulative along-gulf wind stress (CWS) based on 33 detected upwelling events in May-September 2007-2013. Red symbols indicate the events off the southern coast and blue symbols the events off the northern coast; circles correspond to the events with pronounced upwelling front (N_UF and C_UF) and triangles the events with gradual decrease of temperature towards the coast (N_GD and S_GD). The linear regression lines for southern (solid line) and northern upwelling events (dashed line) are shown.

Figure 7. Characteristic distributions of temperature and salinity along the ferry route Tallinn-Helsinki with coastal upwelling events off the northern coast (a, b) and off the southern coast (c,

d); x-axis shows the distance from the Tallinn Bay (latitude 59.48 N) in km along the meridional transect.

Figure 8. Polar histogram of wind stress vectors (N m^{-2}) based on the wind data from a weekly period before the peak of upwelling events off the Estonian coast on 17-23 August 2010 (left panel) and 5-11 July 2011 (right panel).